Researchers Journal of Science and Technology (REJOST)
https://rejost.com.ng

An environmental assessment and *a priori* implications of field investigations of older MSW at Uyo and Younger MSW at Eket, Akwa Ibom State, southern Nigeria

Inyang, N. E.*, Ehibor, I. U., Ekot, A. E. and Udo, I. G.

Received: December 3, 2023 /Accepted: January 21, 2024

Abstract

Whereas dumpsites are unplanned locations for disposing of waste, sanitary landfills are designed to ensure both environmental preservation and improved quality of life. Over the years, there have been concerns raised about the toxic emissions and leachates that landfills and dumpsites release into air and surface water ecosystems. It is commonly known that leachates from the landfill or dumpsite affect the quality of groundwater in nearby areas through subsurface percolation. This work aims at assessing the environmental impacts and the *a priori* implications of the released leachates from older and relatively younger municipal solid waste (MSW) sites through resistivity and hydro-physiochemical studies. The VES curves evaluated were primarily K (50.0%), HK, Q (21.4%), and A (7.1%). The visible lithological sequence was characterized by leachate dispersion, controlled by the inverse square law. The electro-lithofacies in Uyo MSW site has extremely lower resistivity due to older age than Eket MSW, which comparatively displayed marginally low resistivity values due to its seemingly younger age. The hydro-physiochemical parameters indicate that the dumpsites and their contiguous milieus are highly polluted by leachates. The results of this work indicate that groundwater is highly depleted by leachate contaminations and so residential quarters and buildings requiring groundwater resources should not be encouraged within the enclave of the dumpsites. The study reveals that the use of surface and groundwater resources for irrigation in MSW sites depends on salt adsorption ratio and hardness, which necessitates an annual evaluation for environmental mitigation.

✉ **Nsikak E. Inyang:** dosikes5@gmail.com
Department of Geology, Faculty of Physical Sciences, Akwa Ibom State University, Akwa Ibom State, Nigeria

Keywords: Environment assessment; MSW; leachate; resistivity; Hydro-physiochemical species

1.0 Introduction

Sanitary landfills are engineeringly planned trash disposal sites that ensure environmental protection and increased quality of life, whereas dumpsites are haphazard garbage disposal sites. Concerns have been expressed throughout the years concerning the harmful emissions and leachates emitted by landfills and dumpsites into both the water (surface and groundwater) and air habitats. Leachates from the dump site, as is well known, have an impact on groundwater quality in neighbouring areas via percolation in the subsurface. A secure landfill must include four key components: a bottom liner, a leachate collection system, a cover, and a natural hydrogeologic setting. To limit the possibility of waste seeping into groundwater beneath a dump, a natural setting could be chosen. However, due to paucity of funds, citing of sanitary landfills and dumpsites are done without recourse to the key components. This, therefore, leads to excessive environmental pollution that requires assessment and monitoring in a regular basis.

The health risks and environmental consequences of open garbage disposal have been researched at numerous locations throughout the world (Mor *et al*., 2006; Raji and Adeoye, 2017; George *et al*., 2014; Ibuot *et al*., 2023). Near-surface geophysical measurements offer a cost-effective and nondestructive method of investigating pollutant plumes from landfills (Akpan *et al*., 2013). However, there is evidence that leachates formed at dumpsites continue to have an impact on the environment. The geometry of the polluted plume and its migratory pattern in the area surrounding the dumpsite is required to assist rehabilitation and cleanup activities as needed. Geophysics offers several significant features that make it suited for assessing environmental impact. It is noninvasive and nondestructive, and it can provide continuous subsurface data for a profile. As a result, geophysics is essential for assessing contaminated soil. Several authors have employed geophysical methods such as seismic tomography, electromagnetic and electrical resistivity measurements to map dumpsite pollution in subterranean complex terrains (Rosqvist *et al*., 2011; Yoon and Park, 2002; White *et al*., 2016; Zume *et al*., 2006). Geo-electric and hydro-physiochemical investigations were carried out in this study to assess the dumpsite's environmental impact. The dumpsite contains various inhomogeneous components that are mostly non-biodegradable, allowing for long-term interaction between dumpsite materials, soil, and underlying geological units. Waste disposed of in landfills oxidizes, corrosion of metallic components occurs, and organic matter decomposes, creating and releasing leachates that can damage soil, surface, and groundwater resources, as well as the potability of subterranean water.

Due to the continued industrial development and growing urban population municipalities, numerous wastes are created on a daily basis and dumped at a neighboring dumpsite. The waste is deposited in large quantities and on a daily basis, posing an environmental risk to the surrounding area. Surface and groundwater resources are known to traverse across dumpsite channels that run through the study areas. As a result, the dumpsites receive excessive pollutants on a daily basis, either from a waste dump or from a huge industrial sector, suggesting severe environmental pollution. Furthermore, leaching from the deposited garbage may affect groundwater near dumpsites.

The dumpsites have solid garbage and liquid waste. The dumpsite gets considerable amounts of rubbish on a daily basis (Fig. 1). The liquid and solid wastes are untreated, reflecting the seriousness of waste on the surrounding soil and

environment and hence on the population dwelling within the study area. Using near-surface geophysical approach and laboratory analysis of dumpsite-infested water, this study is aimed to explore relatively older and younger MSW sites to identify and compare the minor and major changes within the underlying rocks that are potentially defiled by leachate in Uyo and Eket MSW sites, respectively.

Fig. 1: Diagrams showing sundry waste materials at Uyo MSW site and Eket MSW site where the survey was carried out.

2.0 Location and Geology of the Study Area

The schematic depiction in Fig. 2 shows that the MSW dumpsite in Uyo is located between longitudes 7.931 and 7.940 °E and latitudes 5.04613 and 5.04658 °N, while the MSW dumpsite under investigation in Eket LGA is located between 7.9310 and 7.9367 °E and latitudes 4.6159 and 4.6164 °N. The sites are flat, with elevations ranging from 10.0 to 50.0 meters (mean: 31.5 meters), reflecting the state and local government areas in which they are located. Due to the effect of the Atlantic Ocean, the study sites include undulating terrain topography that is as high as 200 feet above sea level (Evans *et al*., 2010; George, 2020; Etesin *et al*., 2023; George *et al*., 2023; George and Thomas, 2023 a, b). The state, which is naturally located on Nigeria's coast, has various locations that are defined by pleasant valleys, marshes, swamps, and ravines. The research area and its surrounding regions have a moist tropical climate with two (2) distinct seasons, known as the wet season (April to October) and the dry season (November to

March) (Ekanem et *al*., 2022a).The natural environment is favorable for the residents, which include craftsmen, farmers/agriculturists, industrialists, and traders who are mainly involved in the production of MSW. The mapped area has a yearly mean rainfall of 66 inches, and the clime under study is associated with coastal brackish water swamps, dry land, fresh water swamps, and beaches (Ibanga and George, 2016; George *et al*., 2016 a, b). The Benin Formation, the prominent geology of Akwa Ibom State, is often laden with natural deposits of marine, deltaic, estuarine, lagoonal, and fluviolacustrine materials (George *et al*., 2010; Ekanem *et al*., 2022b). Fine to medium and medium to coarse/gravelly sands are interwoven with small argillites throughout the formation (George *et al*., 2011; Akpan *et al*., 2022). The aquifer is made up of argillaceous geomaterials and partially confined and unconfined sands with certain levels of salinities (George and Thomas, 2023).

Continental flood plain sands and alluvium deposits with suitable permeability and porosity are found in the area (Inim *et al*., 2020). Salt water intrusion into sedimentary aquifers occurs under the fresh water lens, which originates about 5 kilometers from the coast (Umoh *et al.*, 2023b). The Benin Formation, with its defectively sorted continental (fine-medium to coarse) units and gravelly sands, alternates with lignite streaks, argillaceous horizons, and lenses to form the hydrogeological units with the study area and its circuited contiguity, which forms the area's multi-aquifer systems (Obianwu *et al*., 2011b; George *et al*., 2016a; George *et al*., 2017).

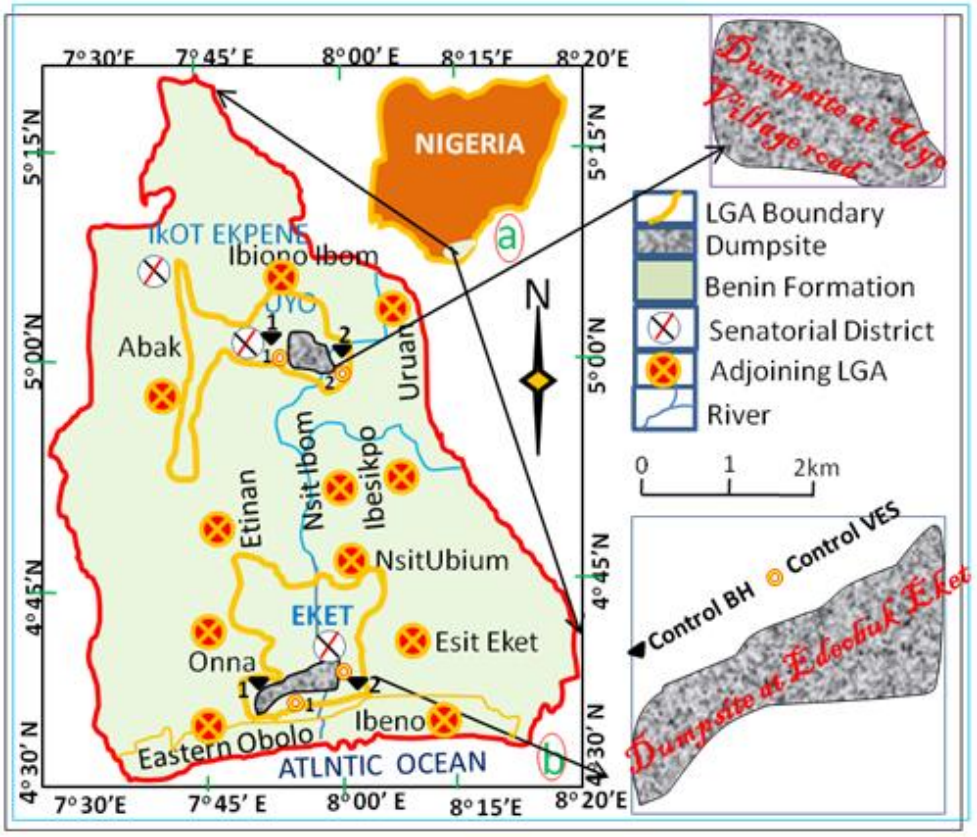

Fig. 2: Schematic diagram showing map of Nigeria and Akwa Ibom State indicating the general geology, open MSW dumpsites in Uyo and Eket, control VES points and boreholes around the dumpsites as well as the contiguous Local Government Areas (LGA)

3.0 Material and methods

3.1 Geophysical data acquisition and analytical techniques

The electrical resistivity approach was chosen for the survey because of water reactions with water-bearing materials, which is a reflection of the bulk change in resistive and conductive nature of subsurface layers (Ibuot *et al*., 2024). At the dumpsite, five vertical electrical sounding (VES) measurements were obtained using the Schlumberger array with a maximum current electrode spacing of 400 m (Fig. 1). A resistivity meter was used to perform VES and ERT operations in the field study. Wenner electrode of constant 5 m separations was utilized for 2D in conjunction with Fig. 3 as described by George *et al*. (2016a, 2021, 2023a) and Obianwu *et al*. (2011a). Applying Fig. 3, the I-D VES data were taken using the Schlumberger electrode configuration. The measurements were made at each surveying point at the Uyo and Eket MSW sites, with a maximum current electrode spread (L) of 400 m for VES and 105 m for ERT, to guarantee appropriate depth coverage suited for the intent of the work. However, offset VES measurements were needed outside the dumpsites where residential buildings were many. The spacing between current electrode separations increases as the depth of current penetration, also referred to as the depth of investigation or depth of burial increases, according to George *et al*. (2016b). The apparent resistivity values for the 1-D VES data and 2-D ERT data were obtained by multiplying the resistance values respectively measured directly from the resistivity meter using Schlumberger and Wenner electrode configurations by geometric constant according to the expressions in Eqs 1 and 2:

$$\rho_{as} = \pi\left(\frac{a^2}{\mathrm{b}} - \frac{b}{4}\right)R_a \qquad (1)$$

where a = (AB/2) is half current electrode spacing and b = MN is spacing between potential electrodes and $R_a = \left(\frac{\Delta V}{I}\right)$, for potential difference ΔV and Current I. The apparent resistivity (ρ_{as}) and geometric factor (G_s) are respectively given by Eqs 2 and 3:

$$\rho_{as} = G_s R_a \qquad (2)$$

$$G_s = \pi\left(\frac{a^2}{\mathrm{b}} - \frac{b}{4}\right) \qquad (3)$$

G_s, which is dependent on the location of the electrodes in the ground was also determined for the Wenner electrode configuration as G_w, given in Eq. 4 after adjusting the electrodes in Fig. 3 to conform to $AM = MN = NB = b = a$: where ρ_{aw} is the Wenner apparent resistivity, R_{aw} is the apparent resistance in the Wenner electrode configuration.

$$\rho_{aw} = 2b\pi\left(\frac{\Delta V}{I}\right) = G_w \times R_{aw} \qquad (4)$$

To generate depth-sounding curves, the apparent resistivity data from the VES survey were graphed along the ordinate axis and the half-current electrode spacing (AB/2) along the abscissa. The VES curve results (Fig. 4) obtained from partial curve matching were utilized to constrain the interpretation using the WINRESIST iteration software. The iteration process in a least squared sense curve matched the measured-observed datasets between 1 and 28 iterations. The goodness of fit was determined through the root-mean square error (RMSE) desired by Uwa *et al*. (2019) and Udosen and George (2018 a, b) to be less than 10%. The 2D electrical resistivity data were processed according to Udosen and George (2018a) into the ERT in Fig. 4 using RES2DINV software package. The interpretations were all constrained

by ground truthing data (borehole data) in order to ascertain sufficiently valid fidelity (George *et al*., 2014; George *et al*., 2022a). The results in Table 1 showcase the primary geo-electric indices (1-D resistivity values, geologic unit's depths of burial and layer thicknesses) of the subsurface lithology. Table 1 also shows VES location coordinates, number of layers that current penetrated as well as the curve types deduced. The method of data collection has a convenient interpretational technique. The VES technique has high dynamic range and is highly robust in resolving the vertical properties within economic aquifer systems (George *et al*., 2022b; Asfahani *et al*., 2023). Again, the constant electrode separation technique (Wenner) has the capacity to resolve robustly the horizontal layering of the lithostratigraphy of the subsurface. The results of these techniques can lay bare the effect of leachate on the electrical properties vertically and horizontally (George *et al*., 2016c; Thomas *et al*., 2020).

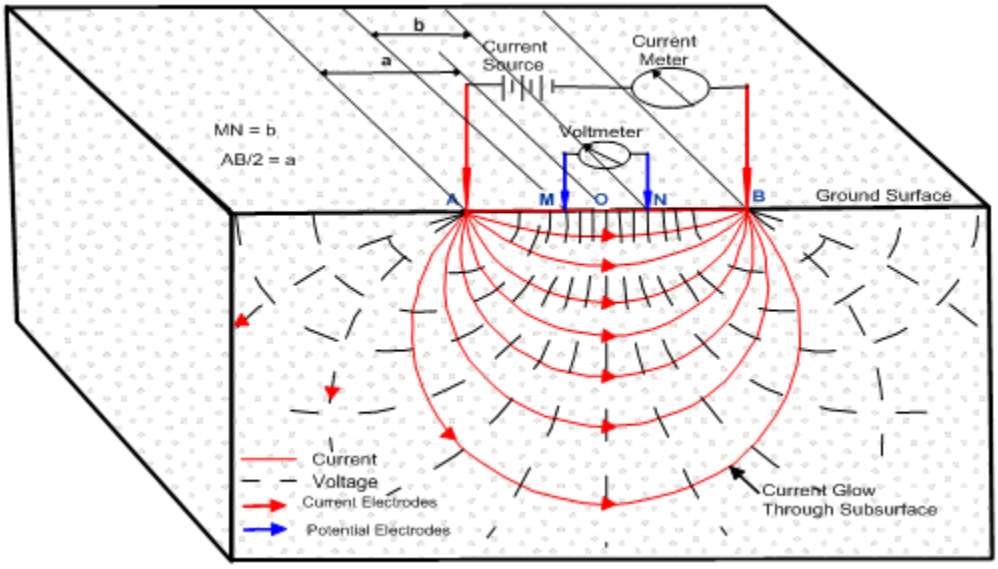

Fig. 3: Diagram schematically illustrating the arrangement in geo-electrical resistivity operation

3.2 Geo-hydrophysiochemical technique

Aside from the geophysical technique, which provides geologically continuous information about subsurface electrical facies changes, water samples collected at and away from MSW sites were collected close to the VES points and analyzed in the laboratory for the physiochemical properties of leachate-infested groundwater. VES points 1-5 and ERT points 1-4 were measured at the MSW sites in Eket and Uyo, respectively (see Fig. 1). VES and ERT were recorded as UV1-UV5 and ERT-U1-ERT-4, respectively, at the Uyo dumpsite. Similarly, in the Eket dumpsite, the VES were coded as EV1-EV5, while the ERT were coded as ERT-E1-ERT-4. Five surface water samples designated WS1-WS5 were collected and analyzed at the Uyo MSW site, whereas two water samples (WS1 and WS2) were collected and analysed in Eket. A sample of water from each borehole was examined at each of the two control sites. The physical characteristics of surface and aquifer interstitial water - temperature, pH, electrical conductivity (EC), alkalinity (AK), DO, COD, BOD, and total dissolved solids (TDS) were ascertained through the analysis of groundwater samples.

Additionally, the geochemical species for the cations of the heavy metallic ion concentrations of Fe, Pb, Mn, Cu, Ni, Cd, and Cr were evaluated. Even at low concentrations, these cations are toxic or dangerous in water due to their very enormous densities.

Once more, Table 2 shows the non-heavy cations of Na, K, Mg, Ca and NH_3, and NH3 as well as the anions of HCO_3^- , SO_4^{2-} and F^- that were required to meet the goals established.

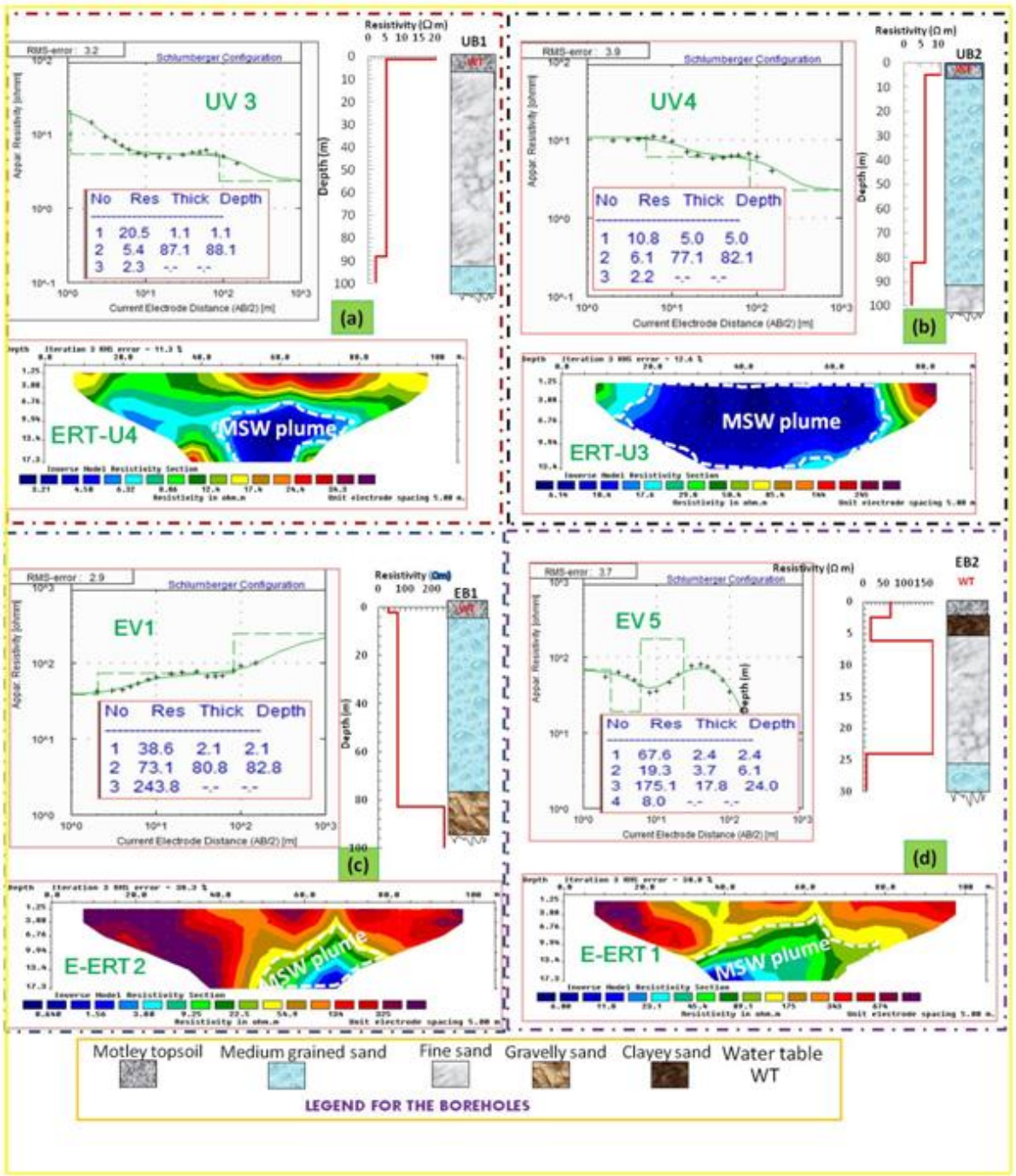

Fig.4: Correlations of some interpreted VES curves, ERT sections and nearby lithology logs: (a) Uyo VES 3 (UV1) near Uyo VES 3 (UV3) and nearby ERT at Uyo (ERT-Uyo A); (b) BH7 (VES5 Versus ERT-B); (c) BH5 (VES8 Versus ERT-C) and (d) BH8 (VES 9 Vs ERT-E).

Table 1: Summary of geo-electric results from computer modeling showing coordinates of sounding points, elevations, and primary geo-electrical indices with bold typeface showing shallower and economic aquifers

VES NO.	Longitude (deg.)	Latitude (deg.)	Elevation (m)	No of Layers	Layer Resistivity (Ohm-m)				Layer thickness (m)			Layer depth (m)			Curve type
					ρ_1	ρ_2	ρ_3	ρ_4	h_1	h_2	h_3	D_1	D_2	D_3	
EV 1	7.933472	4.616333	12.0	3	38.6	73.1	243.8	-	2.1	80.8	-	2.1	82.8	-	A
EV 2	7.933500	4.616389	11.0	3	39.0	61.8	18.2	-	2.1	27.4	-	2.1	27.4	-	K
EV 3	7.933528	4.616444	11.0	3	72.6	173.4	2.9	-	1.2	21.1	-	1.2	22.3	-	K
EV 4	7.937000	4.616139	10.0	3	86.8	257.8	103.2	-	4.5	66.1	-	4.5	70.5	-	K
EV 5	7.936972	4.615889	12.0	4	67.6	19.3	175.1	8.0	2.4	3.7	17.8	2.4	6.1	24.0	HK
EV6C	7.936972	4.618111	10.0	3	424.3	2029.1	767.8	-	1.8	77.6	-	1.8	79.4	-	K
EV7C	7.936917	4.618861	11.0	3	137.4	685.4	285.1	-	4.4	76.3	-	4.4	80.8	-	K
UV 1	7.936528	5.046611	49.0	3	377.3	80.8	5.0	-	4.1	31.4	-	4.1	35.5	-	Q
UV 2	7.936389	5.046167	49.0	4	12.4	1.5	12.4	0.6	2.7	6.4	22.0	2.7	9.1	31.2	HK
UV 3	7.936361	5.046306	49.0	3	20.5	5.4	2.3	-	1.1	87.1	-	1.1	88.1	-	Q
UV 4	7.933583	5.046306	48.0	3	10.8	6.1	2.2	-	5.0	77.1	-	5.0	82.1	-	Q
UV 5	7.936389	5.046222	49.0	4	17.2	3.2	9.4	4.7	3.3	17.9	66.7	3.3	21.2	87.9	HK
UV6C	7.937278	5.046306	49.0	3	254.8	1502.8	850.5	-	2.4	89.4	-	2.4	91.8	-	K
UV7C	7.937417	5.046444	50.0	3	135.9	743.3	219.0	-	7.0	70.5	-	7.0	77.6	-	K
Minimum			10		10.8	1.5	2.2	0.6	1.1	3.7	17.8	1.1	6.1	24.0	
Maximum			50		424.3	2029.1	850.5	8.0	7.0	89.4	66.7	7.0	91.8	87.9	
Mean			31.3		121.1	403.1	192.6	4.4	3.2	52.3	51.6	3.2	55.3	47.7	

3.3 Technique of physiochemical analysis for groundwater samples

Five surface water samples infested with leachates were collected and labelled as WS1-WS5 at the Uyo dumpsite, and two surface water samples were collected and labelled as WS1 and WS2 at the Eket dumpsite in order to estimate the physiochemical compositions of surface and groundwater samples collected at the MSW sites surveyed. Water samples were collected at the dumpsites using 1000-ml polyethylene bottles that had been pre-acid cleaned. They underwent laboratory examinations. Samples that were carried to the laboratory were tested for total alkalinity (the ability of water to withstand pH changes that would make the water more acidic), chemical oxygen demand (COD), and biological/chemical oxygen demand (BOD).

A mercury-filled waterproof thermometer from Fisher Scientific with a temperature range of 0° to 100° C was used to measure the temperature. Every water sample's EC was determined with accuracy to within 0.001s/cm. Using spectrophotometer, the COD -or the quantity of oxygen that may be consumed-was calculated in milligrams per liter of the sample. BOD levels indicated the amount of DO requested or sought by aerobic microbes during organic matter breakdown in MSW water samples. They increased as DO levels decreased as a result of bacteria consuming available oxygen in the water sample. The BOD bottle and standard techniques

were used to calculate the BOD of the water sample. The bottles were completely filled with water to make sure that no air bubbles were trapped in the water samples.

To prevent exogenic processes like vaporization, the plastic tops on the bottles were sealed, and appropriate procedures were followed to guarantee that there was no agitation throughout the transport of the material to the laboratory. This standard procedure was followed by Rana et al. (2018) and Sharma et al. (2020), who kept the samples cold until the laboratory study. The American Public Health Association's (APHA, 2005) guidelines were used to evaluate the physiochemical features.

The measurements of major cations such as Ca^{2+}, Mg^{2+}, Na^{+}, NH_4^{+} and K^{+} were achieved through the use of inductively coupled plasma mass spectrometry (AAS) Model, TECHCOMP (Version: AA6000), while HCO_3^{2-}, SO_4^{2-}, Cl^{-} and F^{-} were determined using the colorimetric or titrimetric method in the analytical Laboratory. All ion species were measured in mg/l except for pH and EC (S/cm). Table 2 shows the lowest, maximum, average, and standard deviation (SD) and their accompanying coefficients of variation of the analyzed physiochemical species, as well as their statistical systematization.

The inductively coupled plasma mass spectrometry (AAS) Model, TECHCOMP (Version: AA6000), was utilized to measure important cations like Ca^{2+}, Mg^{2+}, Na^{+}, NH_4^{+} and K^{+}. In the analytical laboratory, the colorimetric or titrimetric approach was employed to determine HCO_3^{2-}, SO_4^{2-}, Cl^{-} and F^{-}. Except for pH and EC (S/cm), all ion species were measured in mg/l. The examined physiochemical species gave minimum, maximum, average, standard deviation (SD), and corresponding coefficients of variation displayed in Table 2, along with a statistical breakdown of the data. The following seven heavy metallic ion concentrations in part per million or mg/l $(Ni^{2+}, Cr^{2+}, Cd^{2+}, Pb^{2+}, Cu^{2+}, Mn^{2+}$ and $Fe^{2+})$ were evaluated using the standard procedure with the help of the samples that had been prepped using the Gregg (1989) specified Atomic Absorption Spectrophotometers.

3.4 Groundwater pollution index (GPI)

The groundwater pollution index (GPI) was calculated using the average values of two control boreholes: one located approximately 161 meters from the MSW dumpsite at Uyo (BCU) and the other located approximately 215 meters from the Eket MSW dumpsite. This allowed for the observation of the leachate spread from the MSW sites. In order to determine the relative contributions of different physical and chemical facies, the GPI assessment was conducted in compliance with Subba Rao (2012).The estimated species were pH, ELC, TDS, Na^{+}, K^{+}, Mg^{2+}, Ca^{2+}, Cl^{-}, SO_4^{-2}, HCO_3^{-2}, F^{-} and NH_4^{+}. Using the species, an estimate of the general quality of drinking water wells within the dumpsite enclave was made. The following procedures were included in the Subba Rao (2012) approach, which was used to calculate the GPI:

Step 1: A relative weight (RW) of 1 to 5 was given to each species' quality according to the degree to which it affected the drinking water's overall quality. According to Kamaraj *et al.* (2021), the highest RW "5" was given to F^{-}; SO_4^{-2} and Cl^{-}, which have the most noticeable effects while the lowest RW "1" was assigned to parameters that have the least effects (K^{+} and

HCO_3^{-2}). Additionally, pH, TDS and Na^+ were assigned RW "4", while Mg^{2+}, Ca^{2+} and NH_4^+ were assigned RW "2" (Table 3).

Step 2: The parameter of the weight (WP) was calculated.

Step 3: By using the following equation, Eq. 5, the weight parameter (WP), or the ratio of each measured chemical water quality relative weight $\left(\sum RW\right)$ to the total of all relative weights, was calculated:

$$WP = \frac{RW}{\sum RW} \quad (5)$$

Step 4: Utilizing Eq. 6, the concentration status $\left(SOC\right)$ was calculated by dividing the chemical variable concentrations $\left(C_i^n\right)$ for each groundwater sample by the associated drinking water quality criteria $\left(DWQC\right)$.

$$SOC = \frac{C_i^n}{DWQC} \quad (6)$$

Step 5: In step five, WP and SOC were used to calculate the overall quality of groundwater (OQG) for drinking purposes, according to equation 7:

$$OQG = WP \times SOC \quad (7)$$

Step 6: The GPI was computed by adding up all of the OQG values (Eq. 8) in order to verify the effect of contaminants on groundwater quality:

$$GPI = \sum OQG \quad (8)$$

The five pollution potential levels of GPI are as follows, according to Subba Rao et al. (2018), Subba Rao and Chaudhary (2019), and Kamaraj et al. (2021): insignificant pollution level (GPI< 1.0); low pollution level (GPI: 1.0 to 1.5); moderate pollution level (GPI: 1.5 to 2.0); high pollution level (GPI: 2.0 to 2.5); and very high pollution level (GPI > 2.5).

3.5 Soil water irrigation indices using SAR and TH

Soil nutrients, plant production, agricultural yield, and soil texture are all influenced by the chemical makeup of groundwater. Ameen (2019) examined the water from the MSW sites using the total sodium adsorption ratio (SAR). The SAR measures the concentration of sodium (Na) in saturated soil paste water relative to calcium (Ca) and magnesium (Mg). The amount of calcium and magnesium divalent cations in soil water samples, expressed in milliequivalents per liter, is measured as total hardness (TH). The SAR and TH were calculated using Equations 9 and 10:

$$SAR = \frac{Na^+}{\left(\frac{1}{2}\left(Ca^{2+} + Mg^{2+}\right)\right)^{\frac{1}{2}}} \quad (9)$$

$$TH = 50 \times \left(Mg^{2+} + Ca^{2+}\right) \quad (10)$$

The MSW sites were agronomically described using these indices. To evaluate the effect of the dumpsite on the garden surrounding it, this test was necessary.

4.0 Results and discussion

4.1 Geo-electric results

A series of alterations in the inter- and intra-subsurface lithological facies were shown by the electrical resistivity (ERT) and VES data collected and interpreted at the MSW dumpsites in the LGAs of Eket and Uyo. Contiguous ground-truth data limited the interpretation of geo-electrical data in order to remove pseudoscientific assertions resulting from suppression and equivalency principles, electrical resistivity interpretations, and other sources of

error (Fig. 4). The correlations at both MSW locations showed that there were significant relationships between the ground truth data and the interpreted VES data. These investigations showed that there is a consistent level of quality assurance in the geo-electric interpretation outcomes. As illustrated in Fig. 4, the VES resistivity values form a suite of equivalent geologic units that are identified by curve representations generated from primary geo-electric indices (resistivity, thickness, and depth). A series of high and low resistivities at their maximum current electrode separations revealed that the injected current traversed the underlying lithology from top to bottom. Three to four strata that are clearly distinguished from one another by differences in electrical conductivity and resistivity are indicated by the lithological units that Table 1 delineates both inside and outside the MSW sites.

The following curve type distributions are suggestive of the variations hidden within the estimated geo-resistivity (Table 1), as shown in Fig. 5: At EV1, 7.1% of A $(\rho_1 > \rho_2 > \rho_3)$ and 50.0% of K $(\rho_1 > \rho_2 < \rho_3)$ were present at EV2, EV3, EV4, EVC6, EVC7, UV6C and UV7C. Other types of curves that were evident in the study areas were 21.4% of Q $(\rho_1 < \rho_2 < \rho_3)$ at UV1, UV3, and UV4 and 21.4% of HK $(\rho_1 > \rho_2 < \rho_3 > \rho_4)$ at EV5, UV2, and UV5.

Changes in electrical conductivities and facies are reflected in the types of curves that differ between topsoil and bottom soil where current has penetrated.

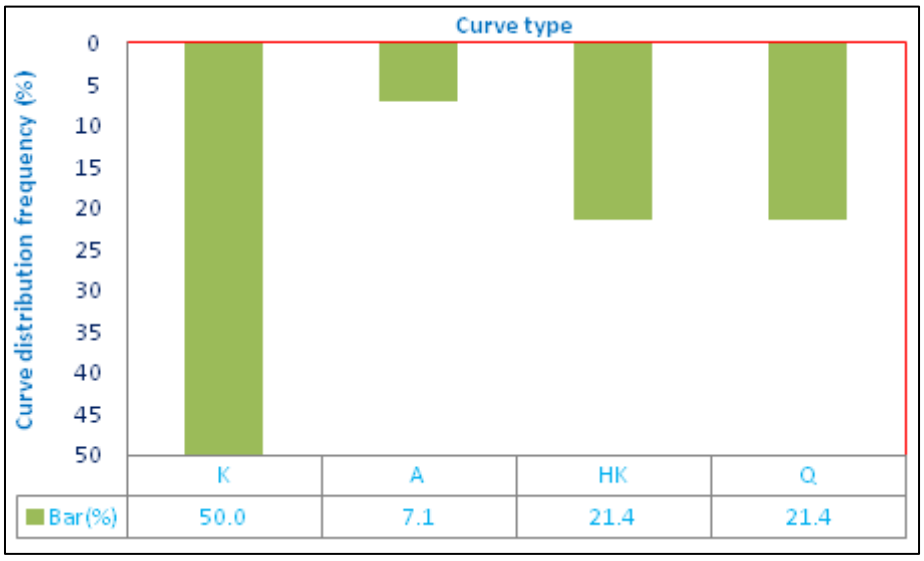

Fig. 5: Resistivity curve distribution frequency showing the curve types that dominate the study areas

The layers' fundamental geo-electric characteristics also differ significantly. Throughout the investigated area, layer 1 resistivities varied from 10.8 to 424.3 Ωm, with an average of 121.1 Ωm. Additionally, thicknesses and depths showed distinct ranges and averages of 1.1 to 7.0 m and 3.2 m, respectively. Resistivity range and mean values were found for layers 2 and 3, respectively, to be 1.5 to 209.1 Ωm (mean: 43.1 Ωm) and 2. 2 to 850.5 Ωm (mean: 192.6 Ωm). Once more, Table 1 displays spatial distributions for layer 2 thicknesses ranging from 3.7 to 89.4 m (mean: 52.3 m) and 17.8 to 66.7 m (mean: 51.6 m). The resistivity of

Layer 4 ranges from 0.6 to 8.0 Ωm, with an average value of 4.4 Ωm. The thicknesses and depths of layer 4 were inaccessible at the greatest electrode separations. The subsurface lithologies' depths and thicknesses were all in line with comparable research conducted in distant regions outside the MSW sites' enclave (Umoh et al., 2022a). However, as can be shown in Figs. 6 and 7, the resistivity values within the studied MSW sites and their surrounding areas clearly showed a drop in resistivity that seemed to follow the inverse square law. It is believed that as we moved away from the upstream main dumpsites (sink), resistivity gradually increased, with the largest drop occurring at the downstream MSW sites (source). The flow of leachate within the radial enclave of the dumpsites is assumed to be the cause of this particular drop in resistivity within the MSW sites. For the MSW dumpsites in Uyo and Eket, the electrical resistivity tomography (Fig. 4) demonstrated a marked decline in the resistivities of the surficial layers (Inim *et al*., 2020). According to George *et al.* (2014), this suggests that MSW leachate flows into the hydrogeological units' pores, increasing the conductivity of the subsurface interstitial fluids and decreasing their resistivities both vertically and horizontally. The porosity and permeability of the pores in geologic layers determine their ability to filter percolating fluids, even though they act as filters (Obianwu *et al*., 2011a; George *et al*., 2015 a, b). It's also crucial to remember that the sort of rubbish disposed of on the dumpsite and its age have an impact on the gravity of the taints released into groundwater (Nkwachukwu *et al*., 2010). Image maps of the aquifers in the MSW dumpsites of Uyo and Eket reveal that the former is older and more active than the latter, which was shown to have a less severe loss in resistivity as a result of leachate percolation (Inim *et al*., 2020).

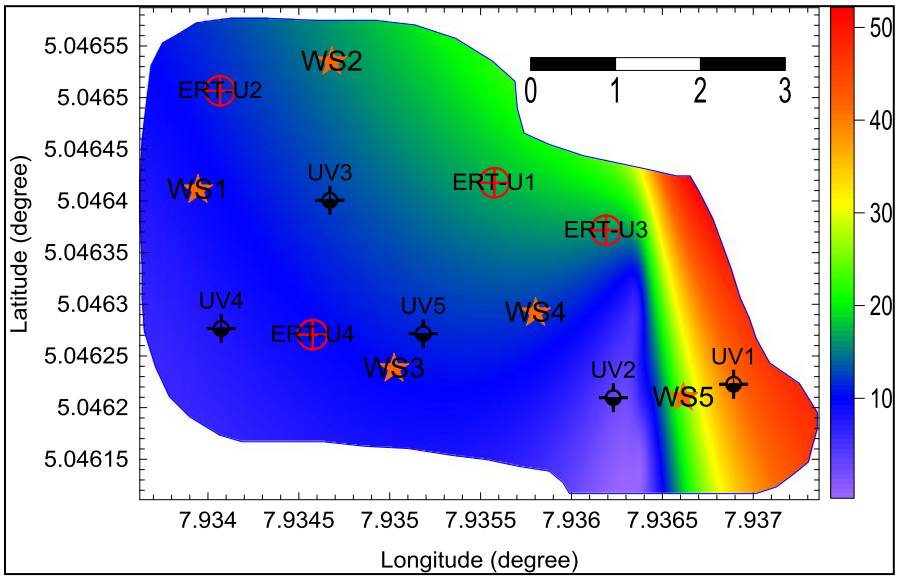

Fig. 6: Image map of the supposed economic aquifer showing drastically reduced aquifer in Uyo MSW site

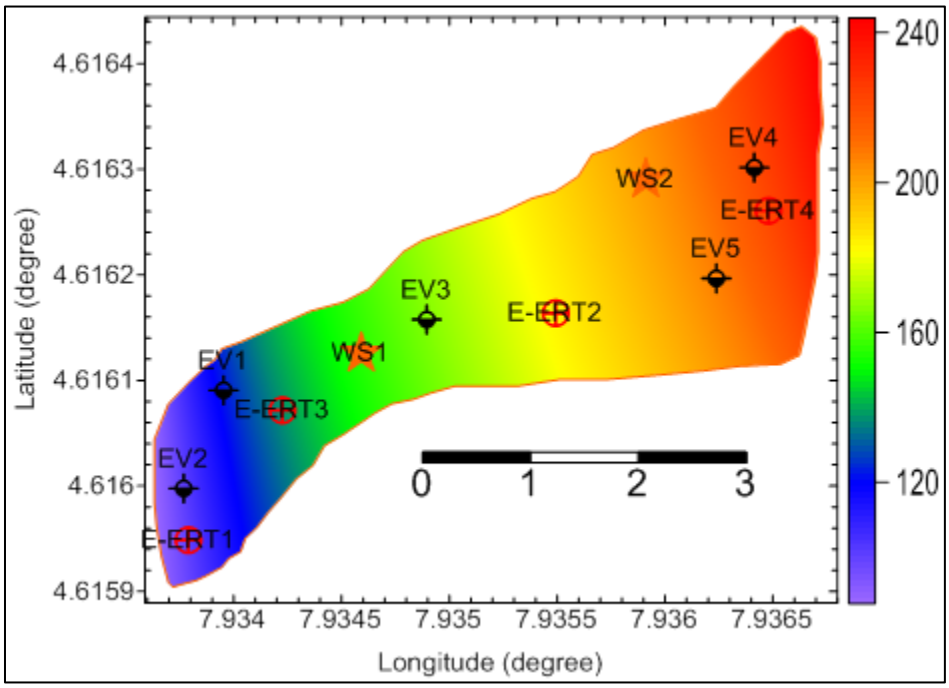

Fig. 7: Image map of the supposed economic aquifer showing drastically reduced aquifer in Eket MSW site

4.2 Geo-hydrophysiochemical results

In order to evaluate the geochemically linked taints in groundwater within the MSW sites, light metal cations, anions, and heavy metallic ions were studied from MSW fluid-infested surface water samples and groundwater samples from nearby boreholes. The physical parameters examined in the water samples analyzed, as shown in Table 2, were pH, with a range of 6.1-8.7 and a mean of 7.67 (std = 0.86); temperature, with a range of 28.8-30.4^{0}C and a mean value of 29.7^{0}C (std = 0.54^{0}C); EC, with an average value of 460.5-2100.1 μS/cm and a mean of 1383.6 μS/cm (std = 669. 2 μS/cm); TDS, with a range of 322.4-1470.1 mg/l and a mean index of 968.5 mg/l (standard deviation = 468.4 mg/l); and alkalinity, with a range of 104.8-1378.9 mg/l and an average of 279.5 (standard deviation = 412.6 mg/l). The water samples exhibit transitory variability in pH (CV: 11.2%), temperature (CV: 1.8%), and EC (CV: 48.4%). The highest level of variability is indicated by alkalinity, with a soaring CV of 147.6%. Furthermore, in comparison to alkalinity, the TDS (CV: 48.4%) is typically less volatile. All freshwater parameters-pH, EC, TDS, alkalinity etc were above WHO recommendations, with the exception of DO, K, Ca, Mg ions and temperature in Table 2 (WHO, 2004). UNICEF (2008) asserts that cooler temperatures affect MSW by preventing the growth of some microorganisms. This prevents garbage from decomposing quickly and prolongs its undigested state. The varied nature of MSW in the surveyed sites suggests that the soil and subsoil fluids (leachate) are not circumneutral but rather move between acidic and basic media, as indicated by the inferred pH value range and average (Thomas *et al*., 2020). The remarkably elevated EC values found in the assessed MSW sites are caused by the leachate that seeped into the nearby surface and groundwater resources. According to Inim *et al*. (2020), this suggests that the total dissolved ions in the water samples are high. The results of the high EC and TDS most likely imply that MSW breaks down quickly in surface water as a solute and that the associated lea

chate then migrates to nearby groundwater resources. High EC and TDS readings, in accordance with Ekström *et al*. (2016), suggest delayed ion exchange between water and geogenic minerals, or the presence of quickly soluble geologic rocks and minerals. Due to the CV of 121.9%, the measured COD, which has a large range of 12.0-1226.1 mg/l and a mean of 317.7 mg/l, is maximally variable. Once again, the computed CV (76.6%) suggests that the BOD, with a range of 2.1-296.0 mg/l and a mean of 100.8 mg/l, is considered to be rather substantially variable. The quantity of organic and inorganic components present is gauged by the COD-BOD ratio. The research MSW sites have an average estimated BOD-COD ratio of 0.32, which suggests that the biological treatment process may be rather sluggish because to the longer time needed for microorganisms to acclimate and aid in degrading activities (Chen et al., 2014). However, by adding seeding (microorganism sludge) to accelerate the breakdown process, the wastewater can be biologically treated, even though the ratio shows that it is not entirely biodegradable because the BOD-COD ratio does not fall between 0.92 and 1.00 (Chen et al., 2014). The DO and CV (17.9%) indicate that there is no significant difference in DO variability between the two MSW sites, with a range of 2.9-4.9 mg/l and a mean of 3.9 mg/l. The MSW sites had a mean BOD of 5 mg/l and the most elevated value not above 5 mg/l. Thomas *et al*. (2020) and George et al. (2023a) report that the sites are more anoxic (condition of insufficient oxygen) than oxic (condition of sufficient oxygen) (DO > 5 mg/L). The average DO value calculated for the two sites, according to Wang *et al*. (2009), suggests that dissolved oxygen is reduced even to the control boreholes at the Eket and Uyo sites (BCE: 4.9 mg/l and BCU: 4.7 mg/l, respectively). The average abundances of light metal cations in Table 2's surface and groundwater hydro-geochemistry analyses are suggested to be in the following order: $NH_4^+ > Na^+ > Ca^{2+} > Mg^{2+} > K^+$; heavy metals as: $Cr^{2+} > Mn^{2+} = Cu^{2+} > Fe^{2+} > Pb^{2+} > Cd^{2+} > Ni^{2+}$. The order of the anionic average relative abundance is as follows: $HCO_3^- > SO_4^{-2} > Cl^- > F^-$. All the anions, save for the chloride ion, have relative average abundances that are higher than the WHO (2014) limit. Due to the link between the waste source (the dumpsite) and the sink (local groundwater sources), as demonstrated in Figs. 6 and 7, this has already negatively impacted the use of groundwater for drinking, as is typical at MSW sites. Once more, the estimated levels of light metals (cations) were within the WHO guideline, although there seemed to be a markedly enhanced presence of sodium and ammonium ions (Table 2). The concentrations of heavy metals (cations), which are denser than water, were higher than the WHO criterion (Table 2). According to WHO (2014), health issues with the use of groundwater for drinking and agriculture were predicted by the significantly high mean indices of all heavy metals in surface and groundwater resources at the MSW site and their enclave. This is because even slightly higher water quality than what the World Health Organization recommends might have negative effects on physiological health. According to Ibuot *et al*. (2017), geological or human action may be to blame for the rise in inferred hydro-geochemical species concen-trations. It is interesting to note that anthropo-genic causes, which result from the dumping of organic and inorganic materials, are unchangeable, while geogenic components could be the source of heavy metals laden in leachate that spread into nearby groundwater resources and surface water sources (Etesin *et al*., 2023).

Table 2: Statistics for physical and geo-hydro-physiochemical species obtained from water sample analysis

S/N	Parameters	WS1 U	WS2U	WS3U	WS4U	WS5U	WS1E	WS2E	BCU	BCE	Range	Mean	Std. dev.	CV (%)	WHO Standard		
															Fresh	brackish	Saline
1	pH	8.1	8.3	8.7	8.0	7.9	7.8	7.7	6.4	6.1	6.1-8.7	7.67	0.86	11.2	<7.5	7.5-8.5	>8.5
2	Temperature (^oC)	30.1	30,3	30.0	30.4	30. 2	29.8	29.3	29.5	28.8	28.8-30.4	29.7	0.54	1.8	<40	-	-
3	Electrical conductivity ($\mu S/cm$)	1400.8	2063.1	2009.1	460.5	2100.1	1987.9	900.7	770.0	760.1	460.5-2100.1	1383.6	669. 2	48.4	<750	750–1500	>1500
4	TDS(mg/L)	980.6	1444.2	1406.4	322.4	1470.1	1391.5	630.5	539.0	532.1	322.4-1470.1	968.5	468.4	48.4	<500	500-1000	>1000
5	Alkalinity (mg/L)	1378.9	154.3	160.6	136.8	129.9	144.2	145.9	159.9	104.8	104.8-1378.9	279.5	412.6	147.6	20-200	varies	Varies
6	COD(mg/L)	406.7	340.7	406.7	1226.1	395.7	28.9	18.6	12.1	23.7	12.-1226.1	317.7	387.4	121.9	<10	10 -15	>15
7	BOD(mg/L)	111.1	80.3	111.1	296	9.8	4.6	2.7	2.1	3.6	2.1-296.0	100.8	77. 2	76.6	<2	2 - 5	>5
8	DO(mg/L)	3.1	2.9	3.8	3.6	3.9	4.8	3.8	4.7	4.9	2.9-4.9	3.9	0.7	17.9	>5	-	-
9	HCO_3^- (mg/L)	400.3	870.7	600.3	607.9	602.1	543.30	612.0	498.2	540.9	400.3-870.7	578.7	380.5	65.8	<500	500-600	>600
10	SO_4^{2-} (mg/L)	136.7	140.6	191.0	121.90	187.30	170.9	156.6	160.0	177.9	121.9-191.0	160.3	22.4	14.0	<150	150-200	>200
11	Cl^- (mg/L)	120.6	138.3	200.5	188.6	139.4	137.5	169.1	160.8	212.8	120.6-212.8	123.6	33.0	26.7	<200	200-250	>250
12	F^- (mg/L)	1.76	1.98	1.38	1.51	1.49	1.23	1.34	1.55	1.61	1.2-2.0	1.56	0.22	14.1	<1.5	1.5-2.5	>2.5
13	K^+ (mg/L)	31.8	28.50	32.70	19.10	23.99	20.11	19.7	22.9	31.00	19.1-32.7	25.7	5.22	20.3	<30	30-55	>55
14	Na^+ (mg/L)	152.9	191.5	140.3	162.8	100.6	190.8	164.9	156.0	198.77	100.6-198.8	160.0	28.89	18.1	<150	150-200	>200
15	Ca^{2+} (mg/L)	66.9	94.90	67.20	78.90	87.9	15.6	50.7	60.7	98.9	15.6-98.9	67.8	24.58	36.3	<100	100-200	>200
16	Mg^{2+} (mg/L)	40.9	38.60	45.9	32.3	37.0	34.8	67.0	78.1	51.0	32.5-78.1	47.3	14.74	31.2	<50	50-100	>100
17	Fe^{2+} (mg/L)	0.22	0.31	0.49	0.38	0.55	0.26	0.23	0.45	0.61	0.2-0.6	0.4	0.14	35.0	<0.3	0.3-0.5	>0.5
18	Mn^{2+} (mg/L)	0.26	0.65	0.11	4.12	0.39	0.01	0.32	0.400	0.54	0.01-4.12	0.7	1.21	172.9	< 0.05	0.05-0.10	>0.1
19	Cu^{2+} (mg/L)	0.10	0.20	0.32	0.15	0.14	0.30	0.80	1.21	2.00	0.1-2.0	0.7	0.72	102.9	<0.05	0.05-2.00	>2.00
20	Pb^{2+} (mg/L)	0.16	0.22	0.19	0.24	0.21	0.25	0.26	0.46	0.58	0.2-0.6	0.30	0.14	46.7	<0.01	0.01-0.05	>0.05
21	Cd^{2+} (mg/L)	0.004	0.005	0.007	0.006	0.14	0.005	0.006	0.005	0.130	0.004-0.162	0.05	0.07	140.0	<0.003	-	-
22	Cr^{2+} (mg/L)	1.300	2.700	2.005	1.005	2.110	1.600	2.650	1.110	1.145	1.0-2.7	1.74	0.62	35.6	<0.003	-	-
23	Ni^{2+} (mg/L)	0.02	0.01	0.02	0.01	0.02	0.01	0.02	0.01	0.03	0.01-0.03	0.02	0.01	50.0	<0.02	-	-
24	NH^+_4 (mg/L)	2279.1	2410.7	800.9	887.4	610.7	480.8	560.4	500.0	510.8	480.8-2410.7	1066.3	802.5	75.3	0.25-32.5	-	-

4.3 Pearson correlation

The linear connection indexes with values between -1 and 1 are commonly analyzed using Pearson's correlation coefficient. As illustrated in Fig. 8, these indices measure the strength and direction of the relationship between two variables. Water quality in surface and groundwater resources is significantly impacted by extraneous dissolved or suspended species from geogenic and anthropogenic sources with high binary correlations produced by hydro-physiochemical species (George *et al*., 2023 b). Light blue, light green, and red represent the weak, moderate, and strong correlation coefficients between two facies of the hydro-geo-physiochemical species. Strong positive and negative correlations are shown in Fig. 8. There are correlation indices between two species that are hydro-physiochemical. For instance, positive correlations have been found between the following species: COD and Tem, pH and Tem, TDS and EC, and BOD and *COD*, Ca^{2+} and F^{-}, Mn^{2+} versus *COD* and *DO*, Cu^{2+} versus Cl^{-} and *DO*, Pb^{2+} and *DO*, Cd^{2+} and Fe^{2+}, Cr^{2+} and HCO_3^{-}, NH_4^{+} and F^{-} as well as Ni^{+} and Cd^{2+}. The results also lay bare the strongly negative correlations in DO and pH across the research area. *Tem*, Cu^{2+} versus *pH* and *Tem*, Pb^{2+} versus *pH* and *Tem*, as well as NH_4^{+} and *DO*. The pairings of hydro-physiochemical species that exhibit positive and negative moderate correlations: $(\geq 0.6 \text{ but} < 0.7)$ and $(\leq -0.6 \text{ but} > -0.7)$ are also shown in Fig. 8. These correlations are displayed in green, and the correlation indices of $(\geq 0.5 \text{ but} < 0.6)$ and $(\leq -0.5 \text{ but} > -0.6)$, which indicate positively and negatively weak correlations, respectively, are displayed in light green (Fig.8). Concisely, the reasonable correlations are seen in the binary pairs of *pH* verses *EC* and *TDS*, *Do* and *Tem*, Mg^{2+} versus *pH*, Tem, and COD, Mn^{2+} and SO_4^{2+}, Cr^{2+} versus *EC* and *TDS*, NH_4^{+} versus *Alk*, SO_4^{2+}, etc. The results show that the pairs of COD and pH have the strongest weak associations. HCO_3^{-} and *Alk*, Cl^{-} versus *Tem*, *EC*, *TDS* and *Alk*, Mg^{2+} versus *EC* and *TDS*, Cr^{2+} versus *pH* and *DO* as well as NH_4^{+} versus *pH*, *Tem*, Cl^{-}, K^{+}, Fe^{2+}, Cu^{2+} and Pb^{2+} etc. The goal of this work is to quickly ascertain the links between different hydro-physiochemical species. According to Kothari et al. (2021) the positive and negative associations reveal details about the nature and origin of the species, their chemical and physical compositions, and their standalone and combined effects on leachate and the groundwater that the resulting leachate is spread to. With values of 0.5 for certain of the binary correlations displayed in Fig. 8, it is not notable that these binary features dissolve in the surface or groundwater under study. It is practically significant to treat surface and groundwater resources for potability using positive (direct), negative (inverse), infinitesimal, weak, moderate, and strong binary correlation values. Figure 8, which denotes the binary interrelationship of leachate-loaded suspended and dissolved physiochemical species in surface and groundwater resources within MSW sites, exhaustively pinpoints the utility of this study and speaks volumes regarding water quality (Kothari *et al*., 2021).

4.4 Surface and groundwater pollution index (GPI)

Using the six steps proposed by Subba Rao (2012) in the technique to identify GPI, the various hydro-physiochemical features and concentrations were identified, and the various compositional indices specified in Eqs. 5-8 were estimated. Nine (9) water samples (WS) were

used to determine the GPI, and Table 3 displays the assignments and computations of eleven (11) hydro-physiochemical species. Table 3 displays the mean value of 3.62 and the range of 0.03 to 38.10 obtained from Eq. 8, which was used to derive the GPI values for each sample. Subba Rao et al. (2018) and Kamaraj et al. (2021) state that the inferred range in Table 4 varies throughout the MSW sites under study, from a minimal GPI level upstream (sink) to a very high GPI level downstream (source) caused by ammonia. The need of keeping an eye on and combating environmental problems associated with open MSW sites in southern Nigeria's Akwa Ibom State is underscored by this finding. Leachate flows both vertically and horizontally through the subsurface from downstream (dumpsite locations) to upstream (dumpsite contiguous zones), as depicted in Figure 4 and the image maps of aquifer units (Figs. 5 and 6). This poses a significant risk to the groundwater resources that are purported to be drinkable. Given that the water in the wells may be carcinogenic; this situation should act as a wake-up call for environmentalists to step up their efforts to stop new boreholes from being built within the radii that are thought to be adjacent to dumpsites (Sexena *et al*., 2004).

	pH	Tem	EC	TDS	ALK	COD	BOD	DO	HCO_3^-	SO_4^{2-}	Cl^-	F^-	K^+	Na+	Ca^{2+}	Mg^{2+}	Fe^{2+}	Mn^{2+}	Cu^{2+}	Pb^{2+}	Cd^{2+}	Cr^{2+}	Ni^{2+}	NH_4^+
pH	1.0																							
Tem	0.8	1.0																						
EC	0.6	0.4	1.0																					
TDS	0.6	0.4	1.0	1.0																				
ALK	0.2	0.2	0.0	0.0	1.0																			
COD	0.5	0.7	-0.2	-0.2	0.1	1.0																		
BOD	0.5	0.6	-0.3	-0.3	0.2	1.0	1.0																	
DO	-0.7	-0.7	-0.3	-0.3	-0.5	-0.5	-0.5	1.0																
HCO_3^-	0.3	0.3	0.3	0.3	-0.5	0.1	0.1	-0.4	1.0															
SO_4^{2-}	-0.1	-0.4	0.5	0.5	-0.4	-0.5	-0.6	0.5	-0.1	1.0														
Cl^-	-0.3	-0.5	-0.5	-0.5	-0.5	0.1	0.2	0.4	0.0	0.3	1.0													
F^-	0.0	0.3	0.0	0.0	0.4	0.2	0.2	-0.6	0.4	-0.5	-0.3	1.0												
K^+	0.1	-0.1	0.3	0.3	0.4	-0.1	-0.1	-0.2	-0.1	0.3	0.1	0.5	1.0											
Na+	-0.3	-0.4	-0.3	-0.3	-0.1	-0.3	-0.1	0.2	0.2	-0.3	0.2	0.2	0.0	1.0										
Ca^{2+}	-0.1	0.1	-0.1	-0.1	0.0	0.3	0.2	-0.3	0.4	-0.1	0.3	0.7	0.5	-0.1	1.0									
Mg^{2+}	-0.6	-0.6	-0.5	-0.5	-0.1	-0.6	-0.5	0.4	-0.2	0.1	0.2	-0.1	-0.1	0.0	-0.1	1.0								
Fe^{2+}	-0.4	-0.3	-0.1	-0.1	-0.5	0.0	-0.1	0.5	0.0	0.6	0.6	0.0	0.3	-0.3	0.6	0.1	1.0							
Mn^{2+}	0.1	0.4	-0.5	-0.5	-0.2	0.9	0.9	-0.2	0.1	-0.6	0.3	0.1	-0.4	0.0	0.3	-0.3	0.0	1.0						
Cu^{2+}	0.9	0.9	-0.5	-0.5	-0.3	-0.5	-0.5	0.7	-0.2	0.3	0.6	0.0	0.1	0.4	0.2	0.6	0.5	-0.2	1.0					
Pb^{2+}	1.0	0.8	-0.6	-0.6	-0.4	-0.4	-0.4	0.7	-0.2	0.2	0.5	0.0	0.0	0.4	0.2	0.5	0.6	-0.1	1.0	1.0				
Cd^{2+}	-0.4	-0.3	0.1	0.1	-0.2	-0.1	-0.4	0.3	-0.1	0.5	0.2	0.0	0.2	-0.3	0.5	-0.1	0.8	-0.1	0.4	0.4	1.0			
Cr^{2+}	0.5	0.2	0.6	0.6	-0.2	-0.2	-0.3	-0.5	0.7	0.2	-0.2	0.1	0.0	-0.1	0.0	0.0	-0.3	-0.4	-0.3	-0.5	-0.1	1.0		
Ni^{2+}	-0.3	-0.6	-0.1	-0.1	0.1	-0.3	-0.3	0.2	-0.3	0.5	0.4	0.0	0.5	-0.1	0.4	0.1	0.5	-0.3	0.5	0.3	0.7	0.0	1.0	
NH_4^+	0.5	0.5	0.3	0.3	0.6	0.2	0.3	-0.8	0.3	-0.6	-0.5	0.8	0.5	0.1	0.3	-0.4	-0.5	0.0	-0.5	-0.5	-0.3	0.2	-0.2	1.0
Legend	Strongly correlated																							
	Moderately correlated																							
	Weakly correlated																							

Fig. 8: Pearson's correlation coefficients revealing the interrelationship of mean hydro-physiochemical properties in the MSW sites studied

4.5 Irrigation evaluation indices

4.5.1 Geo-hydrophysical and hydro-chemical-based classification indices

According to Table 4 (WHO, 2014), the average total dissolved solids (TDS) in surface and groundwater resources is 968.5 mg/l. As suggested by Kothari et al. (2021) for irrigation, this value is less than the saline water (TDS >

1000 mg/l) needed. Table 4 displays the results of comparing the water samples from the two MSW sites. It reveals that only WS1E, with 322.4 mg/l, had fresh water (TDS < 500) found in the sample.

Table 3: Relative weight, weight parameters, and drinking water quality Standards and estimated GIP and its pollution level

Physiochemical species	Units	(RW)	WP	(DWQS)	Sum of GPI	Pollution level
pH	-	4	0.114	7.5	0.19	insignificant
TDS	mg/l	4	0.114	500	0.24	insignificant
Ca^{2+}	mg/l	2	0.057	75.0	0.12	insignificant
Mg^{2+}	mg/l	2	0.057	30.0	0.25	insignificant
Na^{+}	mg/l	4	0.114	200.0	0.20	insignificant
K^{+}	mg/l	1	0.029	12.0	0.13	insignificant
HCO_3^{-}	mg/l	1	0.029	300.0	0.10	insignificant
Cl^{-}	mg/l	5	0.143	250.0	0.21	insignificant
SO_4^{-2}	mg/l	5	0.143	200.0	0.24	insignificant
F^{-}	mg/l	5	0.143	15.0	0.03	insignificant
NH_4^{+}	Mg/L	2	0.057	1.5	38.10	Very high
Total	-	35	1.000	-	-	-

Fig. 4: Table showing the indices of sodium adsorption ratio (SAR) and the total hardness (TH) in the nine water samples across the MSW sites analyzed

Water Code	SAR	TH (meq/l)
WS1 U	3.6	337.6
WS2U	3.3	398.1
WS3U	3.5	359.3
WS4U	3.6	331.8
WS5U	3.4	373.9
WS1E	4.9	184.0
WS2E	3.3	405.9
BCU	2.6	646.9
BCE	2.2	909.0
Min	2.2	184.0
Max	4.9	909.0
Mean	3.4	438.5
STD	0.7	213.4
CV (%)	20.6	48.7

Remarkably, brackish water is available at WS1U, WS2E, BCU, and BCE, where TDS levels ranged from 500 to 1000 mg/l (WHO, 2017). Analogously, all of the surface water samples from WS2U, WS3U, WS5U, and WS1E in Uyo and Eket were saline (TDS > 1000 mg/l). According to Ibuot *et al*. (2017), the amount of TDS in the leachate loaded with MSW is correlated with the variety of biodegradable and non-biodegradable wastes released at the

locations. According to Freeze and Cherrey (1979), water samples from the MSW locations that were tested were deemed to have TDS levels that were genuinely adequate for irrigation. This is because irrigation water needs to be brackish or saline in order to enhance agricultural productivity. Saxena *et al*. (2004) report that the water samples were evaluated for irrigation usage based on electrical conductivity (EC). Thus, at WS4U (250-750 μs/cm), the water sample is good, showing 11.1%. Water samples from WS2U, WS3U, and WS5U make up 33.3% of the total, whereas samples from WS1U, WS1E, WS2E, BCU, and BCE make up 55.6% (Table 4).

According to this finding, numerous tests must be carried out to prove the effectiveness of irrigation water before it is deployed (Hwang *et al*., 2017). In most of the water samples in Table 4, there is a comparable high degree of salinity risk, which may have an impact on crop fertility and yield. Toth (1999) noted that ion exchange reactions and evaporation are responsible for the observed increase in EC values.

4.5.2 Total hardness (TH)

With a mean of 438.5 mg/l, total hardness (TH) in the water samples analyzed using Eq. 9 ranged from 184.0 to 909.0 mg/l. Table 9 shows that TH had a standard deviation of 213.4 and a coefficient of variation (CV) of 48.7%. It is evident from the CV value that the examined water samples were not uniform. All of the water samples examined for hardness in Eq. 9 have very high hardness (>300 mg/l), with the exception of WS1E, which has 184 mg/l, according to Sawyer and McCarthy (1967). The hydro-geological units that collect the surface leachate-loaded MSW waste and the type of wastes disposed of at MSW sites are assumed to be contributing factors to the extremely high degree of hardness observed in MSW sites and their neighboring groundwater (George *et al*., 2014). As for the observable and astronomical surge in the amount of hardness in almost all of the water samples analyzed, it is thought that the rather fine and medium-grained sands in the aquifer geology contain dissolved Mg and Ca ions. Ibanga and George (2016) state that the water's Ca, Mg, and Fe (Table 4) concentrations can stimulate the rust-producing process and its accumulation in metallic and plastic general-purpose (GP) tanks. Therefore, it is stated by Rawat *et al*. (2018) that hard water binds with soil nutrients, making it more difficult for plants to absorb the necessary amount of water, and that this is why plants have more difficulty absorbing and breaking down hard water than soft water. Crop planters and growers may need to raise their irrigation rate due to the increased hardness of the surface and groundwater at the MSW sites. This will help to reduce the negative consequences of using surface and even groundwater nearby for irrigation.

4.5.3 Sodium adsorption ratio (SAR)

As per Eq. 10, the SAR values in the hydro-geological samples obtained from the MSW sites and their adjacent radial zones were 2.2 and 4.9 at BCE and WS1E, appropriately. The standard deviation was 0.7, the CV was 20.6%, and the mean of this range of values was 3.4. The CV indicates how varied the sites under analysis are. A low SAR (SAR< 26) for MSW locations means that the water samples examined there are suitable for irrigation, according to Richards (1954) and Kamaraj *et al.* (2021). There is an urgent need to lower soil alkalinity for some crops and improve soil structure and texture in order to improve sodium content exchange with other cations, as low SAR values indicate low sodium content in surface water and groundwater (Thomas *et al*., 2020). The circulation of air and water into the soil, which influences crop growth, can be enhanced by using this technique, claim Biswas *et al*. (2002).

4.5.4 Comparative deductions from Uyo and Eket Dumpsites

The outcome of electro-lithological compositions indicates that leachate within Uyo MSW site (> 3 decades in age) has considerably more excruciating effect on the surface and groundwater than the Eket MSW site (< 2 decades in age). This is confirmed by the extremely low resistivity values recorded in the shallow and relatively deeper layers in Uyo than in Eket (Fig. 6, 7 and Table 1).The acquired data, which were analyzed and processed, illustrate more pollutant leakage from the dumpsite toward the adjoining groundwater systems in Uyo than Eket. The results come from the low resistivity values that increase marginally from MSW site toward the adjoining site in Uyo and Eket. The assertion can be confirmed from the available lithological logs in the two MSW sites, which showcased drastic reduction in the bulk resistivity of arenaceous geologic units as if they were argillaceous units. However, the decline in the resistivity of geologic units in Eket seems to be marginally small when compared to Uyo. The reason for this variation in the decline of resistivity values is due to variation in the age, volume nature of waste and level of moisture of the wastes within the dumpsite. Uyo MSW site being older in age has more degrading effect than Eket MSW site that is marginally younger. However, the decrease in the resistivity of the water-bearing horizon even (>150 m) away from the dumpsite in Uyo and (> 200 m) away from dumpsite in Eket indicates groundwater pollution by leachates from the dumped wastes. As deduced from borehole data, the nature of litholgical units in the dumpsites studied and its contiguous milieu presupposes lateral and vertical vulnerability to leachate flow and therefore no potable borehole can be successfully drilled within this enclave.

6.0 Conclusion

An evaluation of MSW sites was conducted in order to critically analyze the effects of leachate released by open dumpsites on the surface water and groundwater within the dumpsites, as well as the contiguous groundwater resources. This involved interpreting geo-electrical technology within the constraints of ground-truth data and hydro-physiochemical analyses. The surface and nearby groundwater resources are impacted by the municipal dumpsites in Uyo and Eket, as indicated by a notable increase in conductivity or decrease in resistivity in the geo-electrical data. The presumed economic and prospective aquifers within a depth range of approximately 20 to 90 m have been found to be predominantly saline and brackish due to the dissolved and suspended elements in leachate. Contiguous boreholes in the MSW sites of Eket and Uyo, which are around 190 kilometers away, have been deteriorated by the open dumpsites. The studied region has motley topsoil, fine grains, medium grains, and gravelly sands, which is consistent with Inim et al. (2020) based on the association between the geo-electrical results and the ground-truth data. According to Ibuot *et al*. (2017), fine- and medium-grained sand comprise the economically viable aquifers within the MSW sites and their environs. K (50.0%), HK and Q (21.4%), and A (7.1%) are the most prevalent VES curve types in the survey area. The discoveries show intercalations of various lithological suites. Thick layers differentiate the survey sites, which have shallow water tables (< 20 m). Geology controls the subsurface movements of leachate at MSW sites, both vertically and horizontally, from the source (downstream) to the sink (upstream). The hydro-physiochemical studies showed a direct or inverse relationship between the presence of particular species in surface and groundwater resources and their occurrence. The average

abundance of light metal cations in the following order set apart the results of hydro-geochemical studies of surface and groundwater resources: $NH_4^+ > Na^+ > Ca^{2+} > Mg^{2+} > K^+$; heavy metals as: $Cr^{2+} > Mn^{2+} = Cu^{2+} > \quad Fe^{2+} > Pb^{2+} > Cd^{2+} > Ni^{2+}$ and the anionic relative average abundance in the order: $HCO_3^- > SO_4^{-2} > Cl^- > F^-$. Moreover, it has been determined that ammonium ions are the most serious cause of water contamination, with other ions appearing to have a minor role. According to Mitra *et al.* (2022), the heavy metals' comparatively large CV indicates that their concentrations in water samples can vary greatly, which can lead to carcinogenic effects in people. The region under study appears to be moderately biodegradable, as indicated by the expected BOD-COD ratio of 0.32. Therefore, in order to expedite the degrading process, this needs to be handled biologically by adding seeding (microorganism sludge) (Chen *et al*., 2014).The total hardness of the MSW sites and the adjacent areas is significantly more than 300 mg/l, making irrigation inappropriate. To reduce the detrimental effects of using surface and even groundwater for irrigation close to MSW sites, crop planters and producers may need to increase their watering rate. Once more, based on their classification, MSW sites appear to have a low SAR (SAR< 26), which indicates that the water samples evaluated there are suitable for irrigation. In order to encourage sodium content exchange with other cations, it is critical to lower soil alkalinity for specific crops and enhance soil structure and texture, as these low SAR values indicate low sodium content in surface water and groundwater (Thomas *et al*., 2020; George *et al*., 2024).

Acknowledgements: We are indebted to our colleagues and postgraduate students in the Department of Geology as well as the Department of Physics and the Geophysics Research Group (GRG) of Akwa Ibom State University, for their assistance during the field data acquisition, analysis and editing of the manuscript.

Ethical statement: Not applicable

Conflict of interest: The authors declare that they have no known competing financial interests or personal relationships that could have appeared to influence the work reported in this work.

Consent statement: All the authors have agreed and consented to the contents of the manuscript.

Data availability Statement: The data that support the findings of this study are available from the corresponding author, upon reasonable request.

References

Akpan, A.E., Ugbaja, A.N. & George, N.J. (2013). Integrated geophysical, geochemical and hydrogeological investigation of shallow groundwater resources in parts of the Ikom-Mamfe Embayment and the adjoining areas in Cross River State, Nigeria. *Environ Earth Sci* **70**, 1435–1456. https://doi.org/10.1007/s12665-013-2232-3.

Akpan, .M.J., George, N.J., Ekanem, A., Ekong U.N (2022). Petrophysical appraisal and 3-D structural interpretation of reservoirs in an Onshore Niger Delta Field, Southeastern Nigeria, International Journal of Energy and Water Resources, https://doi.org/10.1007/s42108-022-00218-9.

Ameen, H. A. (2019). Spring water quality assessment using water quality index in

villages of BarwariBala, Duhok, Kurdistan Region, Iraq. Appl Water Sci (9:176). https://doi.org/10.1007/s13201-019-1080-z.

APHA. (2005). Standard Methods for the Examination of Water and Wastewater (21st ed.). Washington, DC.: American Public Health Association/American Water Works Association.

Chen, B., Wu, H., and Li, SFY (2014). Development of variable path length UV-VIS spectroscopy combined with partial-least-squares regression for wastewater chemical oxygen demand (COD) monitoring. Talanta, 120:325–330.

Ekanem, A. M., Ikpe, E. O., George, N. J., Thomas, J. E. (2022a). Integrating geoelectrical and geological techniques in GIS-based DRASTIC model of groundwater vulnerability potential in the raffia city of Ikot Ekpene and its environs, southern Nigeria. Int J Energy Water Res. https:// doi. org/ 10. 1007/ s42108- 022- 00202-3.

Ekanem, K. R., George, N. J., Ekanem, A. M. (2022b). Parametric characterization, protectivity and potentiality of shallow hydrogeological units of a medium-sized housing estate, Shelter Afrique, Akwa Ibom State, Southern Nigeria. Acta Geophysica 70 (2): 879 – 895.

Etesin, U.M., George, N.J, Ogbonna, I.J, Akpan, I.O. (2023). Source Identification and Variation in the chemical Composition of Rainwater in the Coastal and Industrial Areas: A Case Study of Ikot Abasi, South-Eastern Nigeria. Earth Sciences Malaysia, 7(1): 55-63.

Evans, U.F., Akpan, A.E., George, N.J., Obot, I.B. and Akpan, N.I. (2010). A Study of the Superficial Sediments and Aquifers in Parts of Uyo Local Government Area, Akwa Ibom State, Southern Nigeria Using Electrical Sounding Method. E-journal of Chemistry India, 7 (3), 1016-1022.

Freeze, A. R., Cherrey, J. A. (1979). Groundwater. Prentice-Hall, New Jersey.

George N. J., Ibuot J., C., Obiora D. N. O.(2015a). Geoelectrohydraulic parameters of shallow sandy aquifer in Itu, Akwa Ibom State (Nigeria) using geoelectric and hydrogeological measurements, Journal of African Earth Sciences, Egypt, 110, 52-63, http://dx.doi.org/10.1016/j.jafrearsci.2015.06.006.

George N. J., Ubom A. I. and Ibanga J.I. (2014). Integrated approach to investigate the effect of leachate on groundwater around the Ikot Ekpene Dumpsite in Akwa Ibom State, South-eastern Nigeria, *International Journal of Geophysics*, *Hindawi Publishing Company*, 2014: 1-10 (http://dx.doi.org/10.1155/2014/174589).

George N.J., Akpan A. E., Udoh F. Evans (2016a). Prediction of geohydraulic pore pressure gradient differentials for hydrodynamic assessment of hydro-geological units using geophysical and laboratory techniques: a case study of the coastal sector of Akwa Ibom State, Southern Nigeria_, Arabian Journal of Geosciences, 9(4), 1-13.

George N.J., Ibanga, J.I. & Anietie I. Ubom (2015b). Geoelectrohydrogeological indices of evidence of ingress of saline water into freshwater in parts of coastal

aquifers of Ikot Abasi, southern Nigeria, Journal of African Earth Sciences, Egypt, 109, 37– 46, http://dx.doi.org/10.1016-/j.jafrearsci.2015.05.001.

George, N. J., Akpan, A. E. and Ekanem, A. M. (2016b). Assessment of textural variational pattern and electrical conduction of economic and accessible quaternary hydrolithofacies via geoelectric and laboratory methods in SE Nigeria: a case study of select locations in Akwa Ibom State. Journal of Geological Society of India 88(4), 517–528. https://doi:10.1007/s12594-016-0514-6.

George, N. J., Ekanem, A. M., Ibanga, J. I., and Udosen, N. I., (2017). Hydrodynamic Implications of Aquifer Quality Index (AQI) and Flow Zone Indicator (FZI) in groundwater abstraction: A case study of coastal hydro-lithofacies in South-eastern Nigeria. Journal of Coastal Conservation. https://doi.org/10.1007/s11852-017-0535-3.

George, N. J., Obiora, D.N, Ekanem, A. M. and Akpan, A.E. (2016c). Approximate relationship between frequency-dependent skin depth resolved from geoelectromagnetic pedotransfer function and depth of investigation resolved from geoelectrical measurements: A case study of coastalformation, southern Nigeria, Journal of Earth System. Science, India, 125 (7), 1379–1390, DOI: 10.1007/s12040-016-0744-4.

George, N.J. (2020). Appraisal of hydraulic flow unit sand factors of the dynamic sand contamination of hydrogeological units in the littoral zones: a case study of Akwa Ibom State University and its Environs, Mkpat Enin L.G.A, Nigeria. Journal of the International Association for Mathematical Geosciences. https://doi: 10.1007/s11053-020-09673-9.

George, N.J., Agbasi, O.E., Umoh, A.J., Ekanem, A.M., Ejepu, J.S., Thomas, J.E & Udoinyang, I.E. (2023). Contribution of electrical prospecting and spatiotemporal variations to groundwater potential in coastal hydro-sand beds: a case study of Akwa Ibom State, Southern Nigeria. *Acta Geophys.* **71**, 2339–2357, https://doi.org/10.1007/s11600-022-00994-2.

George, N.J., Akpabio, G.T. and K. M. Udofia. (2010). The Implication of Oil Spillage on the Thermal Properties of Soil Samples in the Niger Delta, Southern Nigeria. *Scholars Research Library*, 4 (4), 64-72.

George, N.J., Bassey, N.E., Ekanem, A.M. Thomas, J.E. (2020). Effects of anisotropic changes on the conductivity of sedimentary aquifers, southeastern Niger Delta, Nigeria. *Acta Geophys.* **68**, 1833–1843. https://doi.org/10.1007/s11600-020-00502-4.

George, N.J., Ekanem, A.M., Thomas, J.E. Harry, T.A. (2022a). Modelling the effect of geo-matrix conduction on the bulk and pore water resistivity in hydrogeological sedimentary beddings. *Model. Earth Syst. Environ.* **8**, 1335–1349. https://doi.org/-10.1007/s40808-021-01161-0.

George, N.J, Ekanem, A.M., Thomas, J.E., Udosen, N.I., Ossai, N.M., Atat, J.G. (2024). Electro-sequence valorization of specific enablers of aquifer vulnerability

and contamination: A case of index-based model approach for ascertaining the threats to quality groundwater in sedimentary beds, HydroResearch 7, 71-85, https://doi.org/10.1016/j.hydres.2023.11.006.

George, N.J, Obianwu, V.I., Obot I.B. (2011). Estimation of groundwater reserve in unconfined frequently exploited depth of aquifer using a combined surficial geophysical and laboratory techniques in the Niger Delta, South-South, Nigeria}, Advances in applied science research, 2 (1), 163-177.

George, N.J., Umoh, J.A., Ekanem, A. M, Agbasi, O.E., Asfahani, J., Thomas, J.E (2022b). Geophysical-laboratory data integration for estimation of groundwater volumetric reserve of a coastal hinterland through optimized interpolation of interconnected geo-pore architecture. *Journal Coastal Conservation* **26**, 56. https://doi.org/10.1007/s11852-022-00902-2.

George, N.J.; Thomas, J.E. (2023a). Groundwater potential and quality assessments of a coastal environment: a case study of the location of Federal University of Technology Ikot Abasi (FUTIA), Akwa Ibom State, Nigeria, Journal of Coastal Conservation 27 (4), https://doi.org/-10.1007/s11852-023-00956-w.

George, N. J. and Thomas, J. E. (2023b). Typification of coastal depositional lithofacies with isophysical and isochemical hydro-sand beds via stratigraphic modified Lorenz plots (SMLP): geohydrodynamical implications and valorization of hydrogeological units. *Acta Geophys*. https://doi.org/10.1007/s11600-023-01160-y.

Gregg, L.W. (1989). Water analysis Handbook. H.A.C.H Company, USA. Pp. 33 – 39.

Hwang, J. Y., Park, S., Kim, H. K., Kim, M. S., Jo, H. J., Kim, J. I., Lee, G. M., Shin, I. K., Kim, T. S. (2017). Hydrochemistry for the assessment of groundwater quality in Korea. J Agric Chem Environ 6:1–29. https://doi.org/10. 4236/jacen.2017.61001.

Ibanga, J. I, and George, N. J. (2016). Estimating geohydraulic parameters, protective strength, and corrosivity of hydrogeological units: a case study of ALSCON, Ikot Abasi, southern Nigeria, Arabian Journal of Geosciences, 9(5), 1-16.

Ibuot J.C., Obiora D.N., Okeke, F.N. and George N.J. (2019). Assessment of impact of leachate on hydrogeological repositories in Uyo, Southern Nigeria, *Journal of Environmental Engineering and Science*, 14(2):97–107. https://doi.org/10.1680/-jenes.18.00014.

Ibuot J.C., Okeke F.N., George N.J., Obiora D.N. (2017). Geophysical and physicochemical characterization of organic waste contamination of hydrolithofacies in the coastal dumpsite of Akwa Ibom State, southern Nigeria, Science & Technology: Water Supply, 17 (6): 1626-1637. doi: 10.2166/ws.2017.066.

Ibuot, J.C., Obiora, D.N. & George, N.J. (2024). Evaluation of geohydraulic response properties of hydrogeological units in Littoral hydro-lithofacies in Uyo,

Southern Nigeria. *Appl Water Sci* **14**, 9. https://doi.org/10.1007/s13201-023-02057-3.

Ikpe, E.O., Ekanem, A. M., and George, N.J., (2022). Modelling and assessing the protectivity of hydrogeological units using primary and secondary geoelectric indices: a case study of Ikot Ekpene Urban and its environs, southern Nigeria, Modeling Earth Systems and Environment.

Inim, I.J., Udosen, N.I., Tijani, M.N., Afia, U.E., George N.J. (2020) Timelapse electrical resistivity investigation of seawater intrusion in coastal aquifer of Ibeno, Southeastern Nigeria, Applied Water Science, Germany, 10, 232. https://doi.org/10.1007/s13201-020-01316-x.

Jimenez-Madrid, A, Martinez-Navarrete, C, Carrasco-Cantos, F. (2010). Groundwater risk intensity assessment application to carbonate aquifers of the Western Mediterranean (Southern Spain). Geodin Acta 23(1–3):101–111. https:// doi. org/ 10. 3166/ ga. 23. 101- 111.

Kamaraj, J. , Sekarl, S., Roy , P.D., Senapathi, V., Chung, S.Y., Perumal1, M., Nath, A.V. (2021). Groundwater pollution index (GPI) and GIS-based appraisal of groundwater quality for drinking and irrigation in coastal aquifers of Tiruchendur, South India, Environmental Science and Pollution Research https://doi.org/10.1007/s11356-021-12702-6.

Karlik, G. and Kaya, A. M. (2001). Investigation of groundwater contamination using electric and electromagnetic methods at an open waste –disposal site: a case study from Isparta, Turkey. Environmental Geology, 40(6), 2001, 725-731.

Kothari, V., Vij, S., Sharma, S., Gupta, N. (2021). Correlation of various water quality parameters and water quality index of districts of Uttarakhand, Environmental and Sustainability Indicators,Vol.9, https://doi.org/10.1016/-j.indic.2020.100093.

Mor S., Ravindra, K., Dahiya, R. P., Chandra, A. (2006). Leachate characterization and assessment of groundwater pollution near municipal solid waste landfill site. Environ Monit Assess., 118(1-3):435-56. doi: 10.1007/s10661-006-1505-7. PMID: 16897556.

Nabegu, A. B. (2010). An Analysis of Municipal Solid Waste in Kano Metropolis, Nigeria *Journal of Human Ecology*, 31(2): pp. 111 - 119.

Nkwachukwu, O. I., Chidi, N. I. and Kanno O. C. (2010). Issues of Roadside Disposal Habit of Municipal Solid Waste, Environmental Impacts and Implementation of Sound Management Practices in Developing Country "Nigeria", *International Journal of Environmental Science and Development*, 1(5), 409 - 418.

Obianwu, V.I., Chimezie, I.C., Akpan, A.E., George, N.J (2011a). Surficial Geophysical Deduction of the Geomaterial and Aquifer Distribution at Ngor-Okpala Local Government Area of Imo State, Southern Eastern Nigeria. Central European Journal of

Geosciences, USA, Vol.3 (4), 368-374. Doi: 10.2478/S13533-011-0011-0033-1.

Obianwu, V.I., Chimezie, C.I., Akpan, A.E., George, N.J. (20211b) Estimation of Aquifer Secondary Hydraulic Parameter Distributions from Surficial Geophysical Measurements of Primary Parameters: a Case Study of Ngor-Okpala Area of Imo State, Nigeria, Applied Physics Research 3 (2), 67, 2011.

Obiora D.N., Ibuot, J.C., George N.J, Solomo, U. O. (2016). Delineation of Groundwater Saturation Indicators and their Distributions in the Complex Argillaceous Geological Units of Ezzra North Local Government Area of Ebonyi State, Nigeria, *Journal of current Science*, , Vol.110 , NO. 4, doi: 10.18520/cs/v110/i4/701-708.

Ogwueleka, T. C. (2004). Planning Model for Refuse Management, *Journal of Science and Technology*, 3(2): pp. 71 - 76.

Raji, W.O., Adeoye, T.O. (2017). Geophysical mapping of contaminant leachate around a reclaimed open dumpsite. Journal of King Saud University – Science , 29, 348–359.

Rana, R., Ganguly, R., Gupta, A. K. (2018). Indexing method for assessment of pollution potential of leachate from non-engineered landfill sites and its effect on ground water quality. Environ Monit Assess 190(1): 46. https://doi.org/10.-1007/s10661-017-6417-1.

Rawat, K.S., Singh, S.K. & Gautam, S.K. (2018). Assessment of groundwater quality for irrigation use: a peninsular case study. *Appl Water Sci*, 8, 233. https://doi.org/10.1007/s13201-018-0866-8.

Rosqvist, H., Leroux, V., Dahlin, T., Svensson, M., Lindsjo, M., Mansson, C., Johansson, S. (2011) Mapping landfill gas migration using resistivity monitoring.Waste and Resource Management 164:3-15

Sawyer, G. N., McCarthy, D. L. (1967) Chemistry of sanitary engineers, 2nd edn. McGraw Hill, New York.

Saxena, V. K., Mondal, N. C., Singh, V. S. (2004). Evaluation of hydrogeochemical parameters to delineate fresh groundwater zones in coastal aquifers. *J Appl Geochem.*, 6:245–254.

Subba Rao, N, Sunitha, B., Rambabu, R., Nageswara Rao, P. V., Surya Rao, P., Spandana, B. D., Sravanthi, M., Marghade, D. (2018). Quality and degree of pollution of groundwater, using PIG from a rural part of Telangana State, India. Appl Water Sci 8:227. https://doi.org/10.1007/s13201-018-0864-x.

Thomas, J. E., George, N. J., Ekanem, A. M**.,** Nsikak, E. E., (2020). Electrostratigraphy and hydrogeochemistry of hyporheic zone and water-bearing caches in the littoral shorefront of Akwa Ibom State University, Southern Nigeria. Environ Monit Assess, 192:505 https://doi.org/-10.1007/s10661-020-08436-6.

Toth, J. (1999) Groundwater as a geologic agent: an overview of the causes, processes and manifestations. Hydro J 7:1–14. https://doi.org/10.1007/s100400050176.

Udosen N. I. and George N.J. (2018a). A finite integration forward solver and a domain

search reconstruction solver for electrical resistivity tomography (ERT), *Modeling. Earth System and Environment*, Switzerland, 4(1), 1-12, DOI 10.1007/s40808-018-0412-6.

Udosen, N. I. & George, N.J. (2018b). Characterization of electrical anisotropy in North Yorkshire, USA using square arrays and electricl resistivity tomography, Geomechanics and *Geophysics for Geo-energy and Geo-resources*, Switzerland, 4(3), 215-233, https://doi.org/10.1007/s40948-018-0087-5.

Umoh, J. A., George, N.J., Ekanem, A.M. and Emah, J.B. (2022a) Characterization of hydro-sand beds and their hydraulic low units by integrating surface measurements and ground truth data in parts of the shorefront of Akwa Ibom State, Southern Nigeria. International Journal of Energy and Water Resources. https://doi.org/10.1007/s42108-022-00215-y.

Umoh, J.A., George, N.J., Ekanem, A.M., Thomas, J.E., Emah, J.B. (2022b) Approximate delineation of groundwater yield capacity and vulnerability via secondary geo-electric indices and rock-water interaction hydrodynamic coefficients in a coastal environment, Researchers Journal of Science and Technology, 2(3): 28 -54.

UNICEF, (2008). UNICEF Handbook on Water Quality. United Nations Children's Fund (UNICEF), New York, USA., Pages: 179. United Nations, 2000. Millennium Development Goals. United Nations, New York, USA.

Uwa, U.E., Akpabio, G.T. & George, N.J. (2019). Geohydrodynamic parameters and their implications on the coastal conservation: A case study of Abak Local Government Area (LGA), Akwa Ibom State, Southern Nigeria, *Nat Resour Res.*, 28(2), 349-367, https://doi.org/10.1007/-s11053-018-9391-6.

Wang Y., Zhang1 X., Feng S., Niu Z., Chen C. (2009). Study on inactivation of iron bacteria isolated from real drinking water distribution systems by free chlorine and chloramine, Annals of Microbiology,59 (2), 1-6

White E., Day-Lewis F., Johnson C.D, Lane, J. (2016) Application of frequency and time-domain electromagnetic surveys to characterize hydrostratigraphy and landfill construction at the Amargosa Desert Research Site, Beatty, Nevada. Symposium on the Application of Geophysics to Engineering and Environmental Problems 2015

Yoon, G.L, Oh H., Park J. (2002) Laboratory study of landfill leachate effect on resistivity in unsaturated soil using cone penetrometer. Environmental Geology 43:18–28

Zume, J. T., Tarhule, A., Christenson, S. C. (2006) Subsurface imaging of an abandoned solid waste landfill site in Norman, Oklahoma. Ground Water Monitoring and Remediation 26:62 – 69